

Extrapolation Properties of the Morse/Long-Range Potential

Alketa Sinanaj^{1*} and Asen Pashov

*Faculty of Physics, Sofia University St. Kliment Ohridski,
bul. J. Boirchier 5, 1164 Sofia, Bulgaria*

E-mail: alketa.sinanaj@uniel.edu.al, pashov@phys.uni-sofia.bg

Abstract

Fitting potential energy curves (PEC) for diatomic molecules becomes a well-established routine confirmed empirically with numerous examples in the literature. One of the questions, which remains still open concerns the extrapolation properties of the potential functions. The experimental PECs virtually always are determined from a limited set of experimental data and this in turns limits the range of internuclear distances where the shape of the potential is unambiguously fixed. Extrapolations are usually unreliable because there is no universal analytic form which parametrizes all possible potentials. The Morse/Long-Range (MLR) potential [1] has been reported to have a built in long-range asymptotic behavior and therefore it is plausible to expect that one can expect good extrapolation properties and even possibility to determine important molecular parameters like D_e or/and C_n from limited set of experimental data. In this contribution we study the extrapolation properties of the MLR potential by using real experimental data.

Keywords: diatomic molecules, potential energy curve, dissociation energy, dispersion coefficients.

*11th International Conference of the Balkan Physical Union (BPU11),
28 August - 1 September 2022
Belgrade, Serbia*

¹ on leave from Faculty of Natural Science, Department of Physics, “Aleksander Xhuvani” University, Elbasan, Albania

* Speaker

© Copyright owned by the author(s) under the terms of the Creative Commons Attribution-NonCommercial-NoDerivatives 4.0 International License (CC BY-NC-ND 4.0).

1. Introduction

First approaches for construction accurate, fully quantum mechanical potential energy curves (PECs) for electronic states of diatomic molecules were published already in 1975-1977 [2,3], and named Inverted Perturbation Approach (IPA). Since then, several scientific groups have followed these ideas and demonstrated successful application of IPA in tens, may be even hundreds of cases (examples can be found in [4-8]). The main feature which makes the various applications different is the mathematical form used to construct given PEC. Most often it is an analytic form, but in [4], a model-free, spline point-wise functions are proposed. Both approaches were demonstrated to have advantages. For example, the spline functions are the only form, successful for electronic states with shelf [9], double minimum [10], or other exotic shapes [11]. The analytic forms however are smoother and rarely show unphysical oscillations.

Often the goal of a spectroscopic study is to find parameters of the electronic state, which are not directly measurable, but determined by interpolation (for example the potential minimum U_e , equilibrium distance R_e) or by extrapolation (the dissociation energy D_e) from the fitted PEC. The last quantity D_e , together with the dispersion coefficients C_6 , C_8 etc., which determine the long-range part of the PEC become important with the advances in the laser cooling and trapping, since this part determines the collision properties of the atoms at ultra-low temperatures.

In many studies D_e , C_6 , C_8 were derived from spectroscopic data and the analyses of their uncertainties have shown that for fitting reliable parameters one needs not only accurate and abundant experimental data, but also physically consistent model for the shape of the PEC at large internuclear distances [12].

In some studies, the long-range part of the PEC:

$$U(R) = D_e - C_6/R^6 - C_8/R^8 - \dots \quad (1)$$

is simply attached to the inner part of the potential curve [12]. Other authors develop analytic forms with built-in long-range behavior, which asymptotically approach (1) as R goes to infinity [1,7,8,13]. The smooth and gradual transition from the analytic inner part to the asymptotic form (1) is expected to provide a physically consistent picture (see discussions e.g., in [13,14]). However, a systematic study of the extrapolation properties of these potential forms is still missing and this is the goal of the present paper. We concentrate on the MLR potentials, and we will study the influence of the type of potential, the number of potential parameters and the composition of the experimental dataset on the uncertainty of the long-range parameters.

2. Methods

As a testing case we choose the empirical potential curve for the ground state of calcium dimer from [12]. The accuracy of this potential curve and especially its long-range part has been confirmed in a series of further studies. In [12], Monte Carlo simulation was used to estimate the uncertainties of D_e , C_6 and C_8 . The inner part of the potential was defined as spline pointwise and for the outer – (1) was applied. This approach offered a lot of flexibility, both sections of the potentials are independent, and their shape is determined mainly through the experimental data. On the other side, the MLR form is entirely analytic. It is smooth and more rigid than the pointwise one so it is plausible to expect that narrower confidence intervals on the long-range parameters will be obtained given the same experimental data.

In [1], the experimental data from [12], were used to derive a series of MLR potentials and the final form recommended by the authors has the same quality as the pointwise PEC [1], with very similar estimate on the long-range parameters. The uncertainties, however, were deduced from the matrix of variances and covariances and it did not consider the possible influence of the realization of the MLR potential. Therefore, in this study we construct a large variety of MLR potentials, using different number of parameters and fit them to the same experimental data as in [12]. The general form of MRL potential is [1,13]:

$$V_{MLR}(r) = D_e \left(1 - \frac{u_{LR}(r)}{u_{LR}(r_e)} e^{-\beta(r) \cdot y_p^{eq}(r)} \right)^2 \quad (2)$$

where

$$y_p^{eq}(r) = \frac{r^p - (r_e)^p}{r^p + (r_e)^p} \quad (3)$$

$$y_p^{ref}(r) = \frac{r^p - (r_{ref})^p}{r^p + (r_{ref})^p} \quad (4)$$

$$\beta(r) = \beta_{MLR}(r) = y_p^{ref}(r) \beta_\infty + [1 - y_p^{ref}(r)] \sum_{i=0} \beta_i [y_q^{ref}(r)]^i \quad (5)$$

$$u_{LR}(r) = \frac{C_{m_1}}{r^{m_1}} + \frac{C_{m_2}}{r^{m_2}} + \dots, \quad (6)$$

and

$$\beta_\infty \equiv \lim_{r \rightarrow \infty} \{\beta(r) \cdot y_p^{eq}(r)\} = \lim_{r \rightarrow \infty} \{\beta(r)\} = \ln \left(\frac{2D_e}{u_{LR}(r_e)} \right) \quad (7)$$

Usually r_{ref} , p , q are fixed parameters, while β_i , D_e , C_m , r_e may be fitted to the experimental data. See [1,13]. Detailed explanation on the fitting procedure may be find elsewhere [13], here we only mention that an initial guess for the potential parameters is needed, and it can be realized by fitting the MLR form to some realistic approximation of the PEC. For example, it could be an RKR potential [13], derived from the experimental data. When constructing this initial potential, usually r_{ref} , p , q are fixed to some reasonable values (see [13], for more details) and kept unchanged when the MLR curve is being iteratively improved.

Since we are going to study the extrapolation properties of the MLR form, we will construct a sufficiently large set of potentials, which describe given set of experimental data within their uncertainty. Then we will examine the distribution of the main long-range parameters D_e , C_6 and if all they fall within a reasonably narrow interval we may deduce, that the extrapolation properties of the MLR form are good. We would like to make it clear, that in this paper we do not study the propagation of the uncertainties from the experimental data to the fitted model parameters. This is a problem which can be solved either by using the matrix of variances and co-variances (as for example in [1, 13]) or via Monte Carlo analyses as in [12]. Here we want to study the ambiguity in parameters like D_e , C_6 coming from different composition of the MLR model, i.e. different r_{ref} , p , q , number of β_i . Similar analyses, but with much fewer MLR models were performed in [1].

Initially we took the pointwise potential from [12], in the range [3.1 Å, 10.8 Å] and fitted various initial MLR potentials using the betafit code from [15], using different combinations of r_{ref} , p , q . All these initial curves were further refined through a nonlinear fitting routine by fitting parameters β_i , D_e , C_m , r_e until the fitted PEC reproduced the 3586 experimental frequencies (with $v'' \leq 38$) within their uncertainties. Since the experimental data have different uncertainties, as a measure of the quality of the fit we used the dimensionless standard deviation σ (see [1,12]). The fitted potential was considered as good, if σ is about 0.62 – 0.64, comparable to the value from

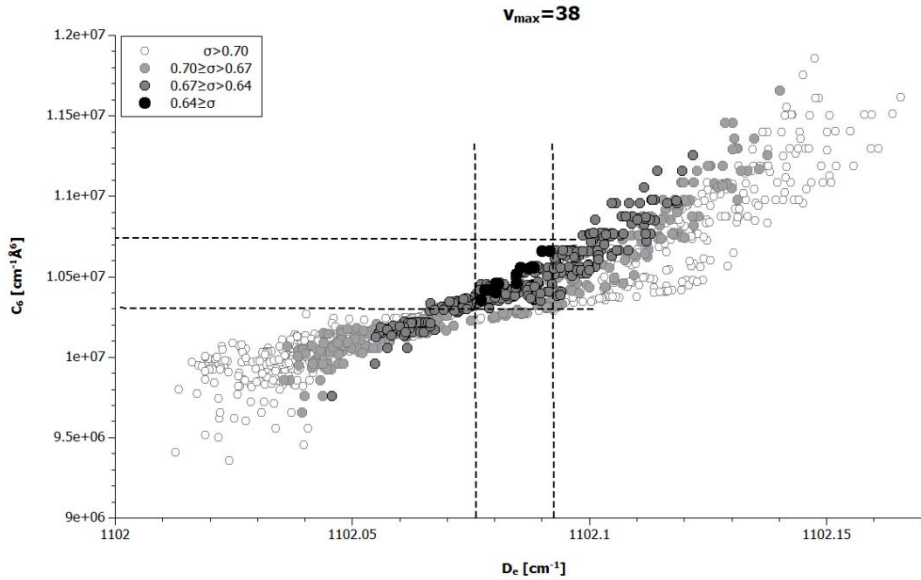
previous studies [1, 12, 13]. In this way about 100 different curves were constructed with $5.15 \text{ \AA} \leq r_{\text{ref}} \leq 5.75 \text{ \AA}$, $5 \leq p \leq 9$ and $3 \leq q \leq 4$. In a similar manner the simulation was repeated for a reduced data set with $v'' \leq 35$.

When using pointwise potential with long-range extension [12], it was shown that the uncertainty of D_e and C_6 strongly depends on the presence of weakly bound energy levels. Increase of v_{max} from 35 to 38 in [12], reduced the uncertainties significantly. If the extrapolation properties of the MLR potential are better, we expect to see small uncertainties of D_e and C_6 even from smaller values of v_{max} .

For every class of potential (defined by r_{ref} , p , q) we started to vary C_6 with small steps each time refining the potential until σ increases above 1.0. In this way we estimated the possible variations of long-range parameters, consistent with the experimental data.

3. Results and Analyses

In Fig.1 we present the distribution of the D_e and C_6 parameters of about 100 classes of MLR potentials for $v_{\text{max}} = 35$ and 38. Each plot contains about 1000 points, resulting from various (D_e , C_6) combinations within a set of r_{ref} , p , q . The shape of the distribution gives an impression about the strong correlation between D_e and C_6 . With different shades of gray, we indicate the dimensionless standard deviation σ . The division between them is somewhat arbitrarily. With black dots we indicate potentials which have $\sigma \leq 0.64$.



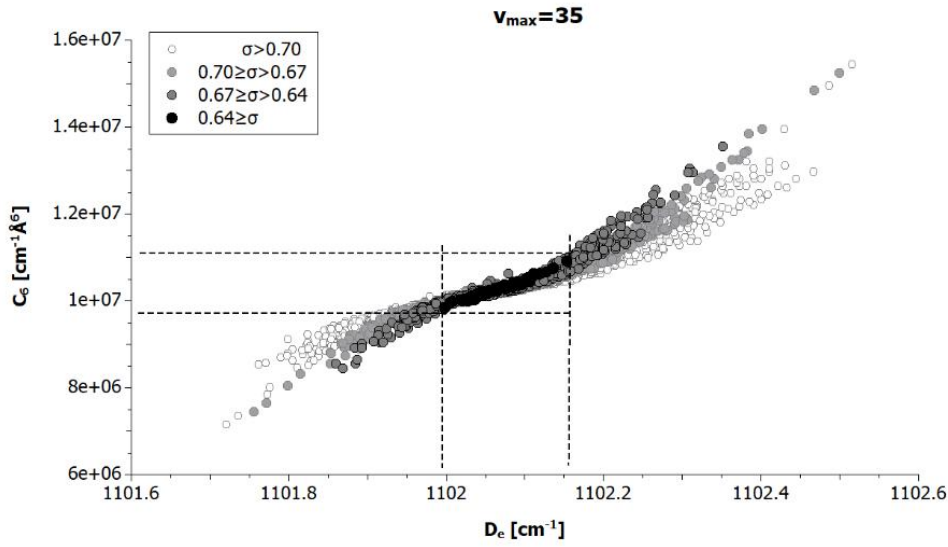


Figure 1: Distribution of the D_e and C_6 parameters of MLR potentials by using different values of r_{ref} , p , q and varying C_6 .

In order to avoid any confusion, we stress the difference between the distributions from Fig.1 and the one from [12]. In [12] the distribution is result of a Monte Carlo simulation by fitting a model to various sets of synthetic experimental data and this simulation shows the uncertainty of the parameters coming from the uncertainties of the experimental data within given model. In Fig. 1 we show distribution which results from different MLR models and the same experimental data.

In [1] all experimental data were analyzed ($v_{\text{max}}=38$) and D_e was estimated to be $1102.076 \pm 0.004 \text{ cm}^{-1}$ (1σ confidence interval) and for C_6 : $(1.032 \pm 0.01) \times 10^7 \text{ cm}^{-1} \text{ \AA}^6$ (1σ). In a later publication [13] even smaller uncertainties were reported, for example $C_6 = 1.046 (\pm 0.003) \times 10^7 \text{ cm}^{-1} \text{ \AA}^6$ (1σ). From Fig.1 ($v_{\text{max}}=38$) we can see that only by changing r_{ref} , p and q one can produce MLR potentials with comparable σ while D_e is varying within approximately $\pm 0.02 \text{ cm}^{-1}$ and C_6 - within $\pm 0.08 \times 10^7 \text{ cm}^{-1} \text{ \AA}^6$. This apparent discrepancy must be resolved. In [1,13] uncertainties coming from the matrix of variances and covariances are reported. They are based on the uncertainties of the experimental data for given realization of the MLR potential. In Table 3 of Ref. [1] the authors show values for D_e and C_6 for few different MLR realizations and their variation significantly exceeds the estimated uncertainties. At the same time these variations fall well within the intervals shown in Fig.1. Therefore, the uncertainties of the final parameters in [1,13] do not account for all possible model dependencies. In fact, in [1] additional analyses were performed to justify the final choice of r_{ref} , p and q (e.g., Fig. 3 in Ref. [1]) and these considerations are reasonable. The goal of our study however is to set an upper limit for the uncertainties coming from the construction of the MLR model itself and to show that regardless of the choice of r_{ref} , p , q and number of β_i parameters the fitted long range parameters will lie within very reasonable intervals. Every physical consideration which allows to limit the variation of these parameters will only further narrow the intervals.

In [12] PEC for the ground state of Ca dimer was determined by applying a very different model function using the same experimental data. For small internuclear distances a cubic spline function was used and for $R > R_{\text{out}}$ the same long-range expression (1) is applied. To estimate the uncertainties of the long-range parameters Monte-Carlo simulations were carried out for $R_{\text{out}} =$

9.4 Å and $R_{\text{out}} = 10.0$ Å. When $R_{\text{out}} = 9.4$ Å the variation of D_0 was estimated and is reported to be ± 0.01 cm⁻¹ (1σ). D_0 is defined as $U(\infty) - E_{v=0, J=0}$, while $D_e = U(\infty) - U_e$. Since the energy of the potential minimum is an unmeasurable quantity and extrapolated, usually D_e is associated with larger uncertainty than D_0 . In [12] the uncertainty of U_e is estimated to be about ± 0.01 cm⁻¹ and it is plausible to estimate the uncertainty in D_e from [12] to ± 0.014 cm⁻¹ which is closer to the estimate of this study. In [12] it is shown that the model also influences the uncertainty of the fitted parameters through the choice R_{out} . Indeed, when $R_{\text{out}} = 10.0$ Å, the uncertainty in D_e increases to about ± 0.017 cm⁻¹.

The advantage of the MLR potential starts to be visible when comparing the distribution of D_e and C_6 for $v_{\text{max}} = 35$ from Fig. 1 and Fig. 5 from Ref. [12]. The pointwise model [12] with $R_{\text{out}} = 9.4$ Å, extrapolates D_e with uncertainty about ± 0.4 cm⁻¹, while the whole set of MLR potentials predicts D_e to within ± 0.08 cm⁻¹. The pointwise model would lead to even larger uncertainty for $R_{\text{out}} = 10.0$ Å. The long-range parameters in [12] are determined mainly from the positions of the very last energy levels ($v''=33-35$) and the values of the pointwise function around the connection point R_{out} . On the other hand, the transition between the short-range and the long-range part in the MLR function is continuous, which introduces more limitations on the possible variations of D_e and C_6 . The advantages of the abrupt transition between two functional forms are discussed in [12]. In brief this is a very flexible way of extrapolation the PEC to large internuclear distances, and it may be used to set an upper limit to the uncertainties. Analytic functions, in principle, may be less flexible and therefore the uncertainties of the long-range parameters may be smaller, but not necessarily more accurate.

4. Discussion

We presented results from the study of the extrapolation properties of the MLR potential form based on comparison between the Ca₂ ground state potential, derived in [1,12,13]. The experimental uncertainty of D_e and C_6 from [1,13] does not consider all possible realizations of MLR, therefore we believe that the reported uncertainties may be somewhat too optimistic. The spline/long-range model from [12] on the other side is too flexible and the reported uncertainties may be too large (for example when $R_{\text{out}} \geq 10.0$ Å). Our analyses show that the predictions of the large variety of MLR models agree quite well both for $\{v_{\text{max}} = 35\}$ and $\{v_{\text{max}} = 38\}$ data sets. So, it is very likely that the MLR model is very suitable, and it offers good extrapolation properties. Further work is needed, however. We plan to study the uncertainties of D_e and C_6 when the data set is reduced to $\{v_{\text{max}} = 30\}$ or even $\{v_{\text{max}} = 25\}$. The binding energy of $v'' = 30$ is about 20 cm⁻¹ with outer turning point about 9 Å and for $v'' = 25$ the binding energy is ≈ 80 cm⁻¹ with outer turning point 7.6 Å. Both these points are below the so called Le Roy radius for Ca₂, beyond which the long-range expansion (1) is assumed to be valid. It is also interesting to check the extrapolation properties in a similar manner for different electronic states and different molecules. Ca₂ is a very pure case with single electronic state, ¹S+¹S atomic asymptote and zero nuclear spin. The ground states of alkali metal diatomic, considered also as simple, have ²S+²S asymptote, non-zero nuclear spin and two electronic states, ¹Σ⁺ and ³Σ⁺, coupled via Fermi contact interaction. Alkaline-earth hydrides, ¹S+²S, offer also relatively simple structure of the ground Hund's case b ²Σ⁺ state. Here, however, the spin-rotation interactions should be considered. For all these cases abundant experimental data exist, so extending the present analyses seems possible.

References

- [1] R. J. Le Roy and R. D. E. Henderson, *Mol. Phys.*, vol. 105, pp. 663-677, 2007.
- [2] W. Hinze and J. Kosman, *J. Mol. Spectrosc.*, vol. 56, p. 93, 1975.
- [3] C. Vidal and H. Scheingraber, *J. Mol. Spectrosc.*, vol. 65, p. 46, 1977.
- [4] A. Pashov, W. Jastrzebski and P. Kowalczyk, *Comput. Phys. Commun.*, vol. 128, p. 622, 2000.
- [5] C. Samuelis, E. Tiesinga, T. Laue, M. Elbs, H. Knöckel and E. Tiemann, *Phys. Rev. A*, vol. 63, p. 012710, 2000.
- [6] J. Y. Seto, R. J. L. Roy, J. Verges and C. Amiot, *J. Chem. Phys.*, vol. 113, p. 3067, 2000.
- [7] J. A. Coxon and P. G. Hajigeorgiou, *J. Mol. Spectrosc.*, vol. 139, pp. 84-106, 1990.
- [8] V. V. Meshkov, A. V. Stolvarov, M. C. Heaven and C. Haugen, *J. Chem. Phys.*, vol. 140, p. (6):064315, 2014.
- [9] A. Pashov, W. Jastrzebski and P. Kowalczyk, *J. Chem. Phys.*, vol. 113, pp. 6624-6628, 2000a.
- [10] A. Pashov, W. Jastrzebski, W. Jasniecki, V. Bednarska and P. Kowalczyk, *J. Mol. Spectrosc.*, vol. 203, pp. 264-267, 2000b.
- [11] A. Pashov, W. Jastrzebski and P. Kowalczyk, "Atomic, Molecular and Optical Physics," *J. Phys. B*, vol. 33, pp. L611-L614, 2000c.
- [12] O. Allard, C. Samuelis, A. Pashov, H. Knöckel and E. Tiemann, *Eur. Phys. J. D*, vol. 26, pp. 155-164, 2003.
- [13] R. J. LeRoy Chapter 6, "Equilibrium Structures of Molecules,," London, J. Demaison and A. G. Csaszar editors, Taylor & Francis, 2011, pp. 159-203.
- [14] J. A. Coxon and P. G. Hajigeorgiou, *J. Quant. Spectrosc, Rad. Trans.*, vol. 151, pp. 133-154, 2015.
- [15] R. J. Le Roy and A. Pashov, *J. Quant. Spectrosc, Rad. Trans.*, vol. 186, pp. 210-220, 2017.